Science of the Total Environment 966 (2025) 178721

Contents lists available at ScienceDirect

Science of the Total Environment

journal homepage: www.elsevier.com/locate/scitotenv

Transitioning from emission source to sink: Economic and environmental trade-offs for CO_2-enhanced coalbed methane recovery of Mannville coal Canada

Haoming Ma [a,b,*], Yun Yang [c,d], Zhenqian Xue [b], Christopher R. Clarkson [c], Zhangxin Chen [a,e,*]

[a] Department of Chemical and Petroleum Engineering, University of Calgary, Calgary, AB T2N1N4, Canada
[b] Department of Petroleum and Geosystems Engineering, University of Texas at Austin, Austin, TX 78712, USA
[c] Department of Earth, Energy, and Environment, University of Calgary, Calgary, AB T2N1N4, Canada
[d] Los Alamos National Laboratory, Los Alamos, NM 87544, USA
[e] Ningbo Institute of Digital Twin, Eastern Institute of Technology, Ningbo, Zhejiang, China

HIGHLIGHTS

- A CO_2-ECBM system analysis simultaneously estimates engineering, economic, and environmental outcomes.
- Deep unminable coal seams are economically viable for CO_2 sequestration while unlock abundant natural gas. unminable coal seams are demonstrated to be economic viable as a emission sink for CO2 sequestrtion and unlock excessive natural gas supply.
- Environmental and economic trade-offs are evaluated to enable the negative emission potentials for the CO_2-ECBM process.

GRAPHICAL ABSTRACT

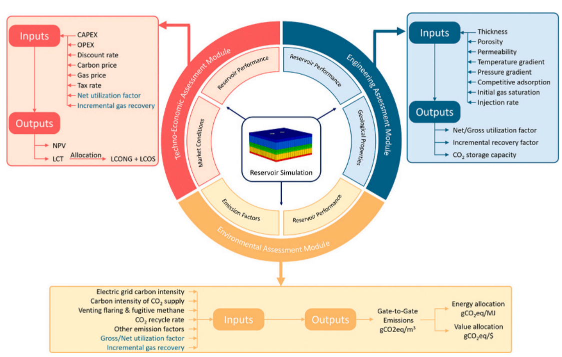

ARTICLE INFO

Editor: Pavlos Kassomenos

Keywords:
CO_2-ECBM
CCUS
System modeling

ABSTRACT

Economically viable and environmentally sustainable geological carbon sequestration (GCS) will be necessitated to mitigate the rising climate change. CO_2-enhanced coalbed methane (CO_2-ECBM) recovery offers a promising solution to address the dual challenges in energy security and environmental sustainability. However, scaling up CO_2-ECBM requires comprehensive multi-perspective understanding at the system level. This work proposes an engineering, economic, and environmental (3E) system analysis framework to evaluate the multi-aspect benefits of CO_2-ECBM, deploying the Mannville coal in Alberta, Canada, as an example. Four key findings are highlighted.

Abbreviations: 3E, engineering, economic, and environmental; ALCA, attributional life-cycle assessment; BHP, bottomhole pressure; CAPEX, capital expense; CBM, coalbed methane; CCUS, carbon capture, utilization, and storage; CDR, carbon dioxide removal; CI, carbon intensity; CLCA, consequential life-cycle assessment; CO_2-ECBM, CO_2 enhanced coalbed methane recovery; CO_2-EOR, CO_2 enhanced oil recovery; CO_2-ESGR, CO_2 enhanced shale gas recovery; CtG, cradle-to-gate; DAC, direct air capture; DCF, discounted cashflow; GHG, greenhouse gas; GtG, gate-to-gate; GWP-20, global warming potential over 20-year; HCPV, hydrocarbon pore volume; IEA, International Energy Agency; LCA, life-cycle assessment; LCOCS, levelized cost of carbon storage; LCOM, levelized cost of methane; LCT, total levelized cost; NPV, net present value; OPEX, operating expense; OPGEE, oil production greenhouse gas emissions estimator; TEA, techno-economic analysis; UF_{gross}, UF_{net}, gross and net utilization factor of CO_2.

* Corresponding authors at: Department of Chemical and Petroleum Engineering, University of Calgary, Calgary, AB T2N1N4, Canada.
E-mail addresses: haoming.ma@austin.utexas.edu (H. Ma), zhachen@ucalgary.ca (Z. Chen).

https://doi.org/10.1016/j.scitotenv.2025.178721
Received 24 November 2024; Received in revised form 27 January 2025; Accepted 1 February 2025
Available online 4 February 2025

Techno-economic analysis
Life-cycle assessment

First, we demonstrated deep unmineable coal seams are reliable CO_2 sinks in that 0.08 kg of CO_2 can be stored per MJ of CBM production. Second, the levelized cost is \$1.19/GJ with a carbon footprint of ~10 gCO_2e/MJ using current technologies. GCS in coal enables carbon offsets due to CO_2 utilization. Third, carbon-neutral and carbon-negative CBM is achievable when CO_2 is point-sourced and from atmosphere, respectively. Lastly, the carbon dioxide removal (CDR) during CO_2-ECBM can generate a trade-off of \$4.7/GJ associated with 8.6 g CDR (a net CDR efficiency of 6.2 %). Economic viable CDR requires a carbon tax of \$175/tCO_2 plus reducing direct air capture (DAC) costs to \$115/tCO_2 or improving DAC efficiency to at least 86 %. This novel integrated framework bridges the gap between energy engineers, economists, and policymakers, unlocking the potential to transform unmineable coal seams from a CO_2 source to a sink.

1. Introduction

Coal still plays a central role in the global energy supply, remaining the largest energy source for electricity generation, cement production and steelmaking (IEA, 2024). Storing CO_2 in coal seams could in part address CO_2 emissions associated with the coal industry and other point-source emitters. Unlike conventional reservoirs, gas storage in coalbed methane (CBM) reservoirs is primarily through adsorption within their microporous structure, which allows for a more secure CO_2 storage compared with other geological porous media (Clarkson et al., 2008). The CO_2-enhanced coalbed methane (CO_2-ECBM) recovery process, applied to deep, unmineable coal formations, provides natural gas to the energy sector while sequestering CO_2 (Clarkson et al., 2008; Moore, 2012). The injection of CO_2 into coal seams can lead to incremental recovery of methane at production wells due to a combination of displacement of methane in the adsorbed phase due to the greater adsorption strength of CO_2, and a partial pressure reduction of methane in the gas phase (Ma et al., 2022; Yang et al., 2022). Until now, this process has only been implemented at the pilot-scale (Yang et al., 2023a). It is possible that the upscaling of CO_2-ECBM will not only provide significant CO_2 storage capacity to meet the drastically rising demand of carbon capture, utilization, and storage (CCUS), but also provide a reliable natural gas supply to meet the energy demand (Ma et al., 2021). In recent years, the industrialization of carbon dioxide removal (CDR) has suggested the possibility of negative-carbon energy sources, which, in turn, could substantially increase demand for geological carbon storage (GCS) (Bui et al., 2018; Tanzer and Ramírez, 2019). Meanwhile, climate policies, such as carbon credits and taxes, and the emissions trading market, have jumpstarted the CCUS industry on a broad scale (IEA, 2023a, 2023b). CO_2-ECBM at scale could become a critical source of future energy supply and element of CCUS commercialization.

Although commercial extraction of natural gas from coal seams is a mature technology in the United States, Australia, China, and Canada, few CO_2-ECBM projects have been implemented because of the cost of deploying CO_2 (Moore, 2012). Several CO_2-ECBM pilot studies, however, have been performed in the United States and Canada since the 1990s, including the Allison Unit and Pump Canyon CO_2-ECBM pilots located in the San Juan Basin of New Mexico, USA, and the Fenn-Big Valley CO_2-ECBM pilot in Alberta, Canada (Gunter et al., 2002). The technical feasibility of this process has been demonstrated through these pilots, but the economic and environmental feasibilities remain unclear; the latter have hampered the application of CO_2-ECBM at the commercial scale. Fortunately, implementation of climate policies enables opportunities for CO_2-ECBM, by taking advantage of the favorable geological storage capacity, while increasing the economic feasibility of the process. For example, a recent field pilot investigation of CO_2 storage in the deep Mannville coal in Alberta has demonstrated technical feasibility, which could potentially generate substantial amounts of carbon tax abatement at the field scale (Yang et al., 2023a).

Despite the technological maturity and climate policy support, a knowledge gap exists in understanding the social-economic trade-offs and the sufficiency of climate policies over the entire CO_2-ECBM supply chain. As such, the emission drivers and mitigation opportunities have not been clearly identified. The existing literature on GHG emissions from upstream fossil fuel extraction predominantly concentrated on crude oil (Cooney et al., 2015; El-Houjeiri et al., 2013; Masnadi et al., 2018a) and natural gas productions (Heath et al., 2014; Littlefield et al., 2019), while studies investigating the carbon footprint of CBM with a specific emphasis on the CO_2-ECBM process remain limited. For example, Liu et al. (Liu et al., 2021) performed life cycle modeling to quantify the GHG emissions of western Canadian natural gas production, comparing the estimates with US studies and estimates from British Columbia, Canada. They revealed that 3.1 to 4.0 gCO_2e/MJ will be generated from upstream natural gas production, smaller than the previous studies (Littlefield et al., 2019). Brandt et al. (Brandt et al., 2022) established an oil production greenhouse gas emissions estimator (OPGEE) to quantify the upstream emissions associated with crude oil extraction methods. This tool has been widely applied to quantify GHG emissions and developing GHG inventories (El-Houjeiri et al., 2013; Kolster et al., 2017; Ma, 2023; Masnadi et al., 2018a; Masnadi et al., 2018b). While it may be possible to use life cycle assessment (LCA) to estimate the GHG emissions associated with CO_2-ECBM, there is insufficient field-scale operational data to support LCA development.

An integrated system analysis can simultaneously address the engineering, economic and environmental (3E) feasibilities of subsurface energy recovery (Abuov et al., 2022; Jiang et al., 2019; Xue et al., 2024a; Xue et al., 2024b) but have not been properly applied to CO_2-ECBM. The reason is that most of the studies were performed for a site-specific case with a primary focus on an economic aspect, such as CO_2 enhanced shale gas recovery (CO_2-ESGR) (Ma et al., 2022) and CO_2-enhanced oil recovery (CO_2-EOR) (Jiang et al., 2019). Although CO_2-ECBM can be technically feasibility, a comprehensive simulation-based framework needs to be established to simultaneously address 3E concerns in supporting large-scale field implementations at their early stage.

To the best of our knowledge, no simulation-based system analysis framework has been created and applied to CO_2-ECBM. In this study, a novel system-level analytical approach is presented, referred to as the 3E analytical framework, to explore the 3E feasibility of CO_2-ECBM by integrating reservoir modeling, techno-economic analysis (TEA) and LCA. The case study of CO_2-ECBM in the Mannville coal in Alberta has been carried out by using this new analytical framework. Economic and environmental parameters with the greatest influence were identified using a sensitivity analysis. In addition, the economic and environmental trade-offs of producing carbon neutral and negative-carbon CBM have been summarized.

The rest of the paper is structured as follows: Section 2 presented an overview of the designed 3E analytical framework, background on the Mannville coal, and the integration of reservoir simulation, TEA and LCA approaches. Section 3 outlined CO_2-ECBM performance from the 3E perspectives and compared it to other subsurface CO_2 enhanced hydrocarbon recovery technologies, such as CO_2-EOR and CO_2-ESGR. The sensitivity analysis and conditions for producing carbon neutral and negative-carbon CBM are discussed subsequently. The economic and environmental trade-offs are elucidated by carbon dioxide removal (CDR) via CO_2-ECBM coupled with direct air capture (DAC). Finally, conclusions are provided and the implications of the proposed 3E analytical framework for CO_2-ECBM are summarized to identify the

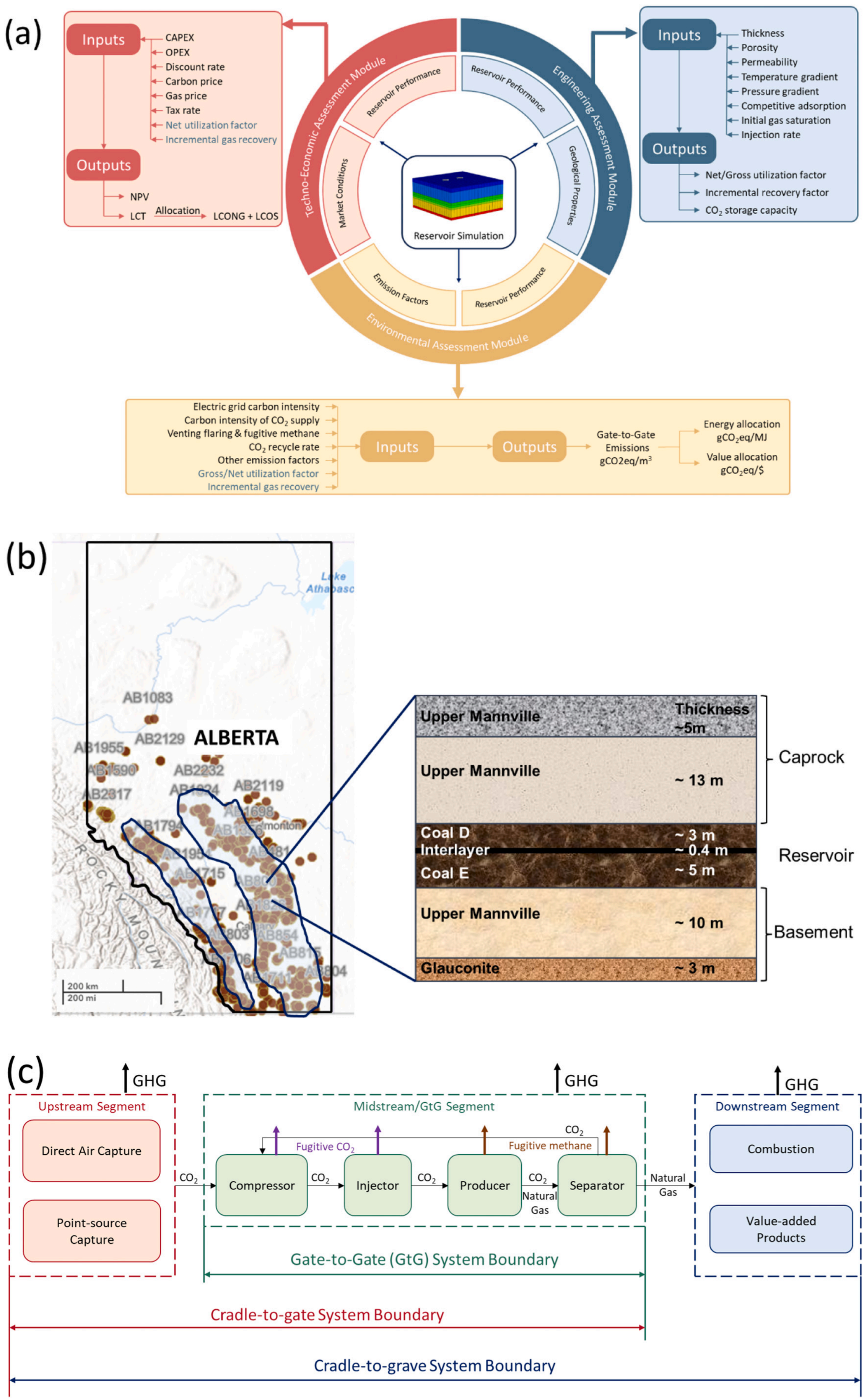

(caption on next page)

Fig. 1. 3E analysis framework of this study. (a) presents the logic structure for CO_2-ECBM system evaluation from the engineering, economic, and environmental perspectives. Six geological and two operational inputs have been collected to the reservoir modeling, six market conditions associated with two results (by reservoir simulation) are deployed to the techno-economic (i.e., discounted cashflow, DCF) model. Five emission factors have been used to develop the environmental assessment model for carbon footprint of CO_2-ECBM associated with reservoir modeling results. A total of seven outputs are expected from the 3E analysis framework (i.e., three from reservoir model, two from DCF model, and two from LCA). (b) highlights the distributions of Manville coal seam in Alberta, Canada (Canadian Institute of Mining, 2024). In this study, we use the three geological formation layers including caprock, CBM reservoir and basement, with a total of seven sub-layers in the reservoir model. More information can be retrieved from our previous study (Yang et al., 2023a) (c) illustrates the system boundaries of CO_2-ECBM, including three segments. The upstream, midstream, and downstream segments refer to capturing CO_2 from either the industrial sources or atmosphere, utilizing CO_2 during the ECBM, and end-use of methane produced by CO_2-ECBM. The cradle-to-gate (CtG) and gate-to-gate (GtG) system boundaries are used in TEA and LCA in later sections.

necessary elements to commercialize CO_2-ECBM.

2. Methodologies

2.1. Study overview

In this work, a 3E analytical framework has been established. The reservoir simulation has been carried out by CMG-GEM such that the performance of CO_2-ECBM and CO_2 storage can be evaluated technically, economically, and environmentally as demonstrated in Fig. 1(a). As stated earlier, the Manville coalbed located in Alberta, Canada with the geological formation highlighted in Fig. 1(b). The reservoir modeling of Manville coalbed has been developed and validated with previous work (Yang et al., 2023a). With the annual predictive CBM production and CO_2 retention by numerical modeling, the techno-economic analysis is conducted by calculating the net present value (NPV) and the total levelized cost (LCT). The carbon footprint can be estimated based on the LCA across the system boundaries, as illustrated in Fig. 1(c). The supply chain of methane as the product from CO_2-ECBM involves three segments, where the upstream, midstream, and downstream segments describe the CO_2 capturing, utilizing CO_2 to recover coalbed methane, and end-use of recovered methane processes, respectively. Table A1 outlined the input parameters involved in this study, where the geological properties are deployed to developing the reservoir model and life-cycle economic and environmental inventories are described to support the TEA and LCA.

2.2. Reservoir modeling

In this section, detail procedures of reservoir modeling are documented based on CMG-GEM, which is a compositional reservoir simulator for the multicomponent, multiphase flow in porous media (Chen, 2007; CMG-GEM, 2020). A dual porosity has been created containing seven vertical layers (see Fig. 1(b)) with a total of 19 × 19 × 9 blocks including natural fractures. Complex physical processes such as diffusion flow in the matrix, competitive adsorption of CO_2 over CH_4, and permeability evolution were characterized in our simulation, which are necessary considerations of unconventional reservoirs in shale and coalbed (Yang et al., 2023a). Diffusion flow in a coal matrix refers to the process where the gas molecules spread out within the coal over time, typically transporting from higher to lower concentration areas (Yang et al., 2023a). Owing to the heterogeneity of coalbed, diffusion coefficient can vary within regions and the matrix can exhibit anisotropic properties (Yang et al., 2022). In this study, we assumed a constant diffusion coefficient for each formation layer. Competitive adsorption of CO_2 over CH_4 describes a physical phenomenon that the absorbed CH_4 molecules are replaced by CO_2 molecules owing to a greater adsorption capacity of CO_2 than CH_4 at the isothermal condition, which can triggered the coal matrix swell and fracture shrinkage, also known as the permeability evolution (Dahi Taleghani et al., 2020; Lu et al., 2023; Xue et al., 2024c). The extended Langmuir model and the Palmer and Higges (P-H) model are adopted to couple the competitive adsorption and permeability evolution mechanisms, consistent with our former investigation (Yang et al., 2023b). Further, the numerical model has been validated with previous work, where a history-match of CO_2 injection had been performed on a field pilot testing project (Yang et al., 2023a). We assume that the matrix and the natural fractures only contain methane or water initially. Two vertical wells (i.e., one producer and one injector) have been drilled with a spacing of 300 m apart from each other at the no flow boundary. The producer was operated under the constant bottomhole pressure (BHP), whereas the injector was operated under the constant flow rate, assuming the injection pressure not exceeding the caprock failure pressure. The life span of the project is assumed to be five years.

The reservoir performance was evaluated from both CBM recovery and geological CO_2 sequestration perspectives, of which three computational outputs are obtained from the numerical model: the incremental recovery factor, effective CO_2 storage, and the CO_2 utilization factor. Eq. (1) describes the incremental CBM recovery factor in percentile by taking a ratio of incremental CBM production over the OGIP, which has been used in CO_2-EOR and CO_2-ESGR prior to this work (Ma et al., 2022).

$$RF_{in} = \frac{P_{in}}{OGIP} \tag{1}$$

where P_{in} is the incremental CBM production in volumetric unit and OGIP refers to original gas in place, both in a volumetric unit. The total gas injection has been normalized to HCPV scale (Eq. (2)) such that the direct correlation between CO_2 utilization and RF_{in} can be revealed (Ma et al., 2022).

$$CO_{2inj,HCPV} = \frac{\sum V_{CO_2,inj}}{V_{HCPV}} \tag{2}$$

where $CO_{2inj,HCPV}$ is the total injected CO_2 in HCPV scale, $V_{CO_2,inj}$ is volumetric CO_2 injected and V_{HCPV} defines the total hydrocarbon pore volume (HCPV).

The gross and net utilization factor (UF_{gross}, UF_{net}) are selected to estimate the effectiveness of CO_2 injection on CBM production, as shown in Eqs. (5) and (6) (Ma et al., 2022). The utilization factors are the foundational inputs for the TEA and LCA analysis, as the UF_{net} provides the estimation of CO_2 purchasing cost, where UF_{gross} can be used to assess the carbon footprint of field CO_2 recycling, which is a carbon intensive process (Cooney et al., 2015).

$$UF_{gross} = \frac{\sum \rho_{CO_2} \times V_{CO_2,inj}}{\sum P_{in}} \tag{5}$$

$$UF_{net} = \frac{\sum \rho_{CO_2} \times \left(V_{CO_2,inj} - V_{CO_2,prod}\right)}{\sum P_{in}} = \frac{R_{CO_2} \times \rho_{CO_2} \times V_{CO_2,inj}}{\sum P_{in}} \tag{6}$$

To conveniently apply both factors to the TEA and LCA framework, we normalized the total injected/retained CO_2 to mass basis by multiplying with the CO_2 density (ρ_{CO_2}) at the corresponding conditions for both equations. Typically, ρ_{CO_2}=1.87 kg/m^3 at the standard condition (NIH, 2024).

2.3. Techno-economic model

Limited existing literature can be retrieved in the context of TEA of CO_2-ECBM. Therefore, we referred to the relevant pioneer studies in the topics of CO_2-EOR and CO_2-ESGR to develop s the discounted cashflow (DCF) model (Abuov et al., 2022; Jiang et al., 2019). In summary, the total project revenue consisted of annually trading produced natural gas plus offsetting or removing CO_2 from either industrial emitters or DAC process by saving the carbon tax in Canada (Alberta Energy Regulator, 2023; Fukai et al., 2016; Government of Alberta, 2024; Hughes et al., 2022; International Energy Agency, 2022b), mathematically presented as Eq. (7).

$$Rev = p_{NG} \times P_{in} + c_t \times UF_{net} \times P_{in} \tag{7}$$

where, p_{NG} is the market price of natural gas in the unit of \$/GJ and c_t is the potential marginal revenue of geological carbon storage, by either offsetting or removing CO_2 depending on the sources, in unit of \$/ton. As a reference, the carbon tax in Canada is announced to rise to CAD 170 (USD 125, as the conversion rate of 2024) by 2035 with an annual increment of CAD 15 (USD 11) (IEA, 2022a). A dynamic c_t has been implemented to the DCF subsequently with a constant growth of USD 10/yr. The total expenditure comprised capital (CAPEX) and operational costs (OPEX), as defined in Eqs. (8) and (9).

$$CAPEX = C_{drilling} + C_{equipment} + C_{land} \tag{8}$$

$$OPEX = C_{CO_2,purchase} + C_{CO_2,transport} + C_{CO_2,recycle} + C_{monitor} + C_{other} \tag{9}$$

$$\begin{cases} C_{drilling} = 328,112 \cdot exp(0.0003D); 0 < D < 1500 \\ C_{drilling} = 0.1418 \cdot D^{1.9107}; 1500 < D < 4000 \end{cases} \tag{10}$$

The drilling cost refers to the expense associated with drill vertical wells, well completion, hydraulic fracturing and day-to-day expenses associated with the operations. The empirical costs are evidenced in the joint associated survey (JAS) reported by the American Petroleum Institute (API) since 1954, and the total cost can be evaluated based on the regression method as Eq. (10) demonstrated (Jiang et al., 2019; McCoy and Rubin, 2008). However, given the high variability of hydraulic fracturing cost, such as proppants and chemicals purchase, geographical locations, regulatory requirements, and labor availability, the actual cost can be substantially beyond the theoretical estimation, which added limitations to this study (Gong et al., 2020). Equipment cost contains the infrastructure installations, including the wellhead, injecting, producing equipment, compressor, separator etc. Cost of land use typically defines the purchasing or leasing of the land according to the local regulations. In this study, we combined the land and equipment cost with a 25 % salvage value by the end of the project lifespan.

The NPV and the levelized cost are two economic benchmarks of the DCF model. The NPV function is defined as Eq. (11) with assuming a constant discount rate (τ^d), income tax rate (τ^s), and the royalty rate (τ^R), where the values can be found in Table A1 (Jiang et al., 2019). A 5-year straight-line depreciation was applied to the DCF in calculating the earnings before interest and tax (EBIT).

$$NPV = -CAPEX + \sum_{i=1}^{i=5} (Rev_i - OPEX_i)(1-\tau^s)(1-\tau^R) \Big/ (1+\tau^d)^i \tag{11}$$

Owing to the dual functionalities (producing CBM and storing CO_2) of the CO_2-ECBM at the system level, we define the levelized cost comprised of two parts, the levelized cost of methane (LCOM) and the levelized cost of carbon storage (LCOCS). The total levelized cost (LCT) of the system is defined in Eq. (12), which is the sum of LCOM and LCOCS. We adopted weighting factors based on the ratio of revenues generated by selling CBM or saving carbon tax to allocate LCT to LCOM and LCOCS, mathematically presented in Eqs. (13) and (14). The allocated LCOM and LCOCS allowed us to conduct comparisons of cost versus market price of natural gas, carbon tax for CBM and CO_2 storage, respectively, according to each functionality.

$$LCT = \frac{\left[CAPEX + \sum_{i=1}^{i=5} OPEX_i \cdot \frac{(1-\tau^s)(1-\tau^R)}{(1+\tau^d)^i}\right]}{P_{in}} = LCOM + LCOCS \tag{12}$$

$$\text{Weighted factor}: \begin{cases} w_{CBM} = p_{NG} \times P_{in}/Rev \\ w_{CS} = c_t \times UF_{net} \times P_{in}/Rev \\ w_{CBM} + w_{CS} = 1 \end{cases} \tag{13}$$

$$\text{Allocation}: \begin{cases} LCOM = LCT \times w_{CBM} \\ LCOCS = LCT \times w_{CS} \end{cases} \tag{14}$$

2.4. Simulation-informed life-cycle emission analysis

The ISO14040/44/67 standardized the procedures of applying LCA into four phases to quantify the GHG emissions for products or engineering activities (ISO14040, 2006; ISO14044, 2006; ISO14067, 2018). Previous studies have successfully quantified the carbon footprint associated with CO_2-EOR or conventional natural gas production, but limited work attempted to understand the GHG emissions along with the CO_2-ECBM process (Abuov et al., 2022; Azzolina et al., 2016; Liu et al., 2021; Masnadi et al., 2018a). In this study, a simulation-informed LCA framework was established to disclose the potential carbon footprint of CO_2-ECBM based on numerical modeling. In this section, the elements of simulation-based LCA for CO_2-ECBM have been outlined as follows.

In this work, we pursue two goals by deploying the LCA framework. First, we attempt to quantify the environmental impact reduction for CO_2-ECBM process based on the case of Manville coalbed. Second, in combining with the TEA, we aim to address the economic cost of minimizing GHG emissions for the CO_2-ECBM, which allows us to perform consistent comparisons with other CO_2 enhanced hydrocarbon recovery options economically and environmentally.

To compare the performance of CO_2-ECBM with other similar technologies, we specify the functional unit of *producing 1 MJ of methane during the CO_2-ECBM associated with the carbon sequestration*. Accordingly, the emission reduction opportunity of the entire process can be quantified and compared with similar techniques, which normally report GHG emissions on an energy basis.

The GHG emissions are estimated across the system boundaries as illustrated in Fig. 1(c). We specifically focus on the CtG, which comprises of the upstream and midstream segments. The downstream segment was excluded because the end-use GHG emission of methane can be substantially differed depending on the utilization purpose, upgrading configurations, and regional constrictions.

The LCA methods can be widely divided into two subcategories, the attributional and consequential LCA methods. The consequential LCA (CLCA) focuses on highlighting the environmental impacts with respect to the adoption of the candidate products or systems, while the attributional LCA (ALCA) directly assesses the environmental impact of the products or systems in a static manner (von der Assen et al., 2014). In this paper, we performed the ACLA as we focus on leveraging the understanding of environmental benefits of the simulated CO_2-ECBM process for Manville coalbed specifically. According to the system boundary definition, the CtG emissions are mathematically presented by Eq. (15).

$$E_T = E_{upstream} + E_{CO_2-ECBM} = \left(E_{capture} - M_{supply}\right) \times R_{CO_2} + E_{operation} \tag{15}$$

The net emission (E_T) contains upstream and midstream emissions, referring to the carbon capturing and CO_2-ECBM process in this context. The upstream emission ($E_{upstream}$) is the emission of supplying unit mass CO_2, typically 1 kg or metric ton (Sleep et al., 2021). This is also known as the carbon intensity (CI) of CO_2 supply, where the positive value indicates CO_2 is sourced from industrial emitters and negative value means CO_2 is removed from air through DAC. By multiplying with the retention factor (R_{CO_2}), the effective geological carbon storage can be

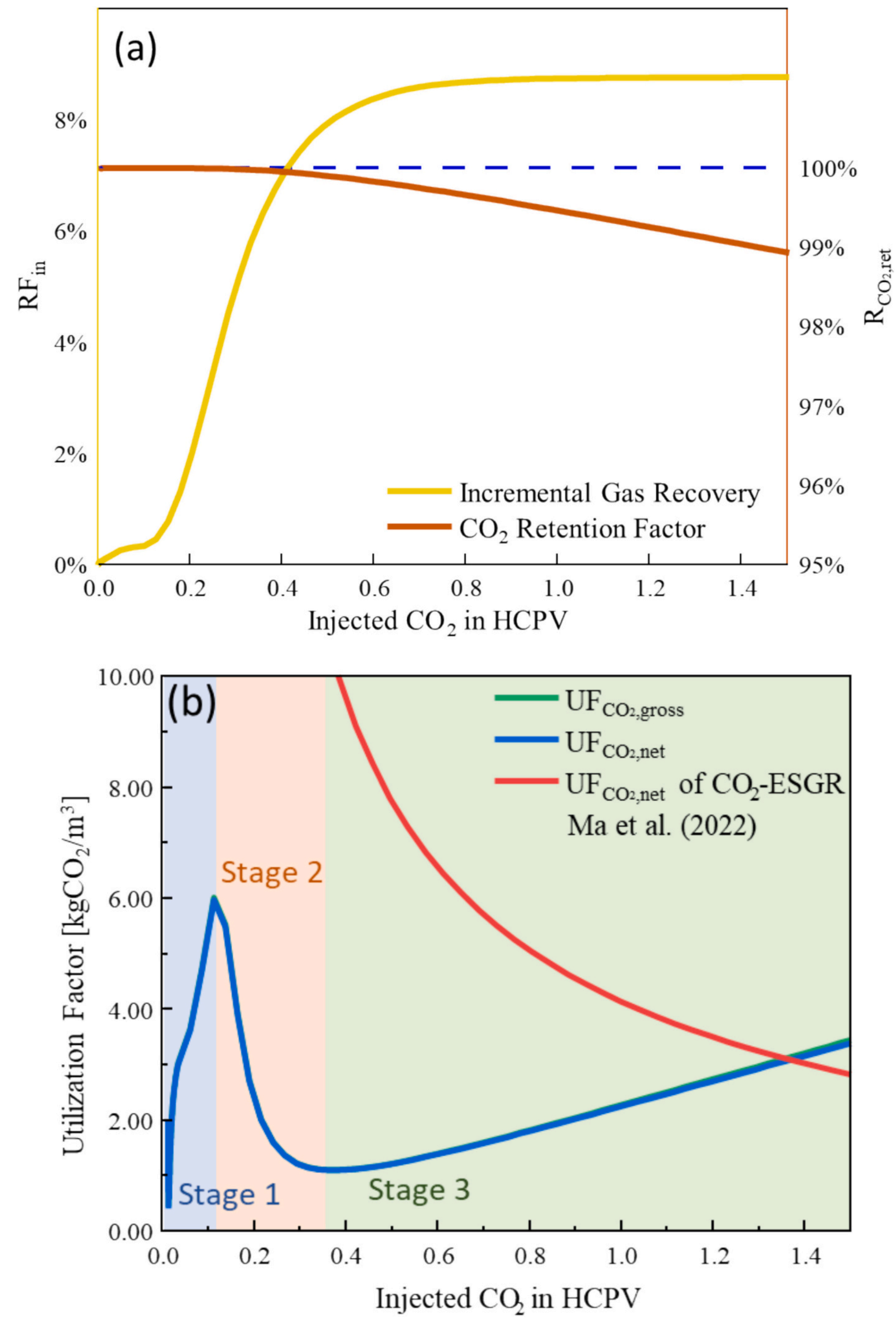

Fig. 2. Engineering performance from the basic reservoir modeling. Both(a) and (b) use CO_2 injection in HCPV scale as the dependant variable (*x*-axis). In detail, (a) presents the incremental gas recovery factor (RF_{in}, left *y*-axis) and CO_2 retention factor (R_{CO_2}, right *y*-axis), representing the performance evaluation from both CBM recovery and geological CO_2 sequestration perspectives. (b) depicts the trends of gross/net utilization factors ($UF_{CO_2,Gross}$, $UF_{CO_2,net}$) with respect to the CO_2 injection in HCPV scale with comparison of our previous study for CO_2-ESGR (Ma et al., 2022). Detail discussion for each stage can be found in the main text below. (c) illustrates the CO_2 storage by mechanisms comparing with our previous study on Barnett shale (Ma et al., 2022). (d) compares the net utilization factor of CO_2-ECBM with CO_2-ESGR and CO_2-EOR with existing studies (Azzolina et al., 2016; Cooney et al., 2015; Ma, 2023; Masnadi et al., 2018a).

calibrated subsequently. The operational emissions ($E_{operation}$) describe all other anthropogenic emissions of the engineering activities such as gas compression, separation, injection, and recycling (Environment and Climate Change Canada, 2023; Environmental Defense Fund, 2015). Gas transportation is neglected in this work as it contributes negligible proportions as long as there is no detected leakage empirically.

In this paper, we assess the global warming potential over 20-year (GWP-20) for the CO_2-ECBM process, as it is reflecting the short-term environmental impact. We use the unit of CO_2e to characterize GWP-20 in the later context. Regarding the methane emissions, we applied a conversion factor 86 to quantify GWP-20 of the leaking methane, because it has much larger global warming impact than CO_2, 86 and 34 times higher than CO_2 over the 20-year and 100-year timeframe, respectively (IPCC, 2023).

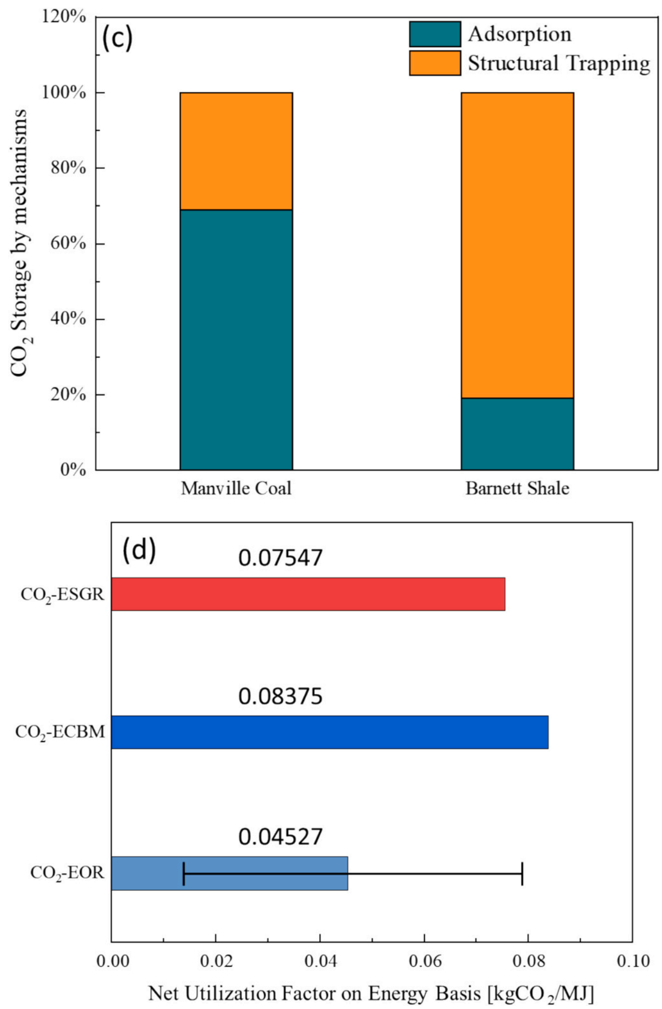

Fig. 2. (*continued*).

3. Results and discussion

3.1. Engineering performance

In this section, the technical performance of CO_2-ECBM has been discussed based on the numerical modeling carried out by CMG-GEM. As stated earlier, the CO_2 injection was normalized to HCPV scale such that the temporal noise can be eliminated. We investigated the RF_{in} and $R_{CO_2,ret}$ to reveal the reservoir performance with respect to the CBM production and effective CO_2 sequestration, respectively, as illustrated from Fig. 2(a). As a result, a total of 8.5 % additional CBM was extracted owing to the utilization of CO_2. Over the 5-year timeframe, 99 % of cumulative injected CO_2 had been successfully stored in the deep coal seam via the structural and adsorptive mechanisms. A CO_2 breakthrough was recorded after the 0.23 HCPV of CO_2 injection, which corresponded to two years and six months of operation evidenced from our compositional reservoir modeling. Differ than other numerical studies of CO_2-EOR and CO_2-ESGR, the $R_{CO_2,ret}$ were greater than other CO_2 enhanced hydrocarbon recovery processes, indicating that better CO_2 storage performance can be expected owing to unique features of the deep coal seam, where adsorption can dominate the geological carbon sequestration. The utilization factors (UF_{gross} and UF_{net}) were plotted and compared with our previous work of CO_2-ESGR as shown in Fig. 2(b). Since approximately all injected CO_2 (i.e., 99 %) can be retained to the reservoir, we noticed that the difference between UF_{gross} and UF_{net} can be negligible. We classified the entire CO_2-ECBM operation into three stages based on the tendency of UF_{net}. In stage one (i.e., blue region in Fig. 2(b)), at the early stage of CO_2 injection, CBM was produced dominantly by the pressure-driven mechanism. The gas production rate was declining with respect to time, and only methane gas content was produced as all injected CO_2 retained to the reservoir by structural trapping. Since the producer and injector were assumed to be operated simultaneously, the *UF* was increasing as CO_2 injected, where the CBM production was not affected by CO_2 injection during this stage. In stage two (i.e., the light pink region in Fig. 2(b)), the *UF* diminished from its max value to reach the minimum with the rapid increase of CBM production. The sharp improvement in the production rate was caused by permeability revolution and competitive adsorption mechanisms, where competitive adsorption was the key reason triggering this observation, especially at the latter time of this stage. The mechanisms of enhanced methane recovery are the same as the CO_2-ESGR process, but with the different magnitude on each mechanism, where competitive adsorption dominates the CO_2-ECBM process owing to the greater adsorptive gas content on coal compared with shale. The *UF* reached its nadir when CO_2 was breakthrough, and gradually grew in stage three, meaning that the CO_2 was stored in absorbed phase, and the methane production was depleted. The UF_{gross} and UF_{net} started apart from each other during this stage along with the CO_2 production. Compared with our previous investigation on CO_2-ESGR, the *UF* was monotonically declining from the positive infinite, where the CO_2 was injected after the gas rate declined to near-zero. In addition, although competitive adsorption was considered in CO_2-ESGR, it had a more substantial impact on CO_2-ECBM in both gas recovery and carbon storage aspects. At the later stage of both operations, the increasing trend of *UF* in CO_2-ECBM demonstrates a

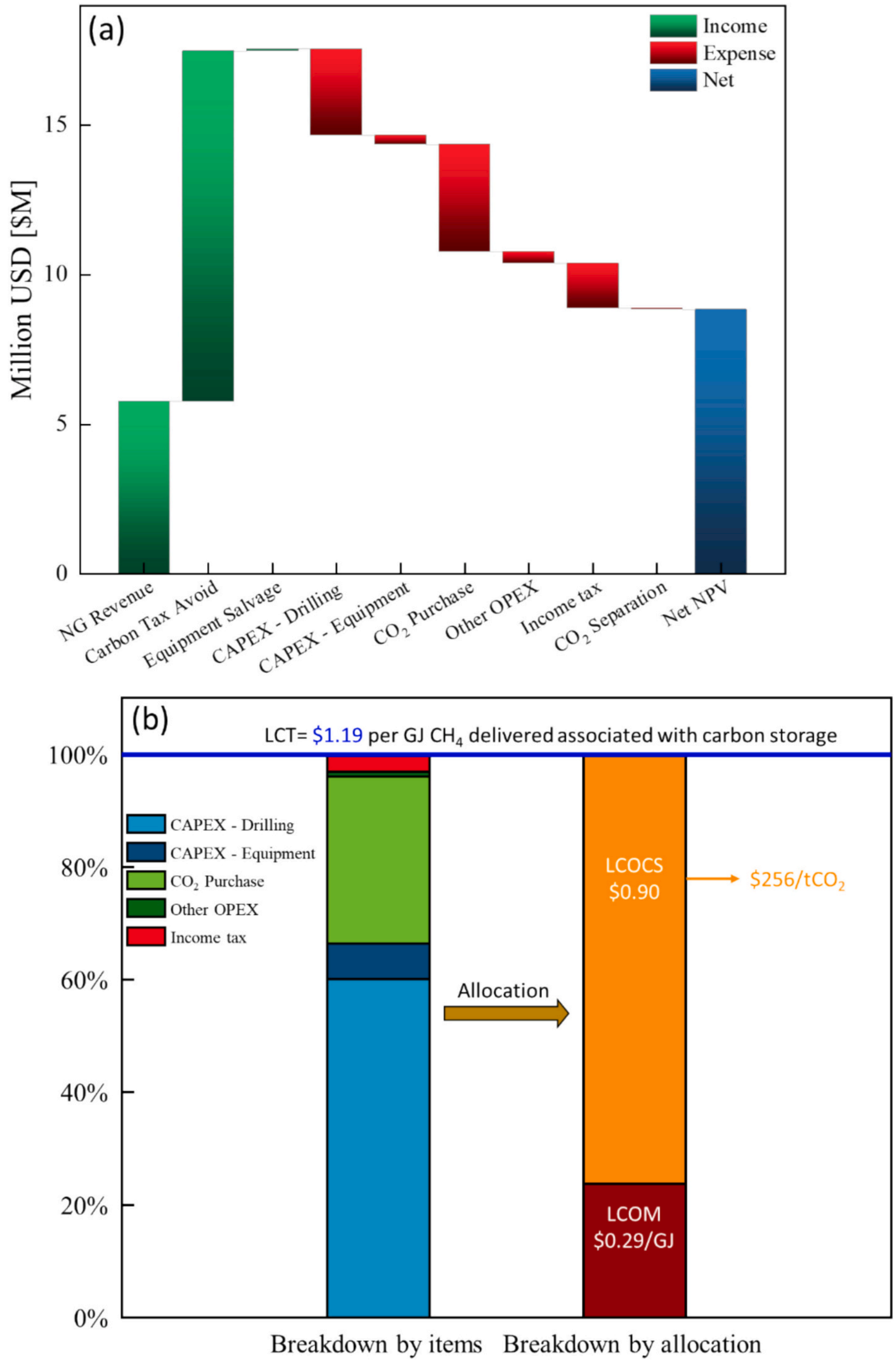

Fig. 3. Breakdown of (a) NPV and (b) LCT on energy basis. (b) allocates the LCT to LCOCS and LCOM with using the value allocation factor by Eqs. (13) and (14).

better capability of CO_2 storage due to the greater adsorption capacity of CO_2 on coal compared with shale. However, a limitation of this work was that the timing of CO_2 injection might be underrepresented in the reservoir model, which contains high uncertainty during the field operation and leading to the increasing *UF* in stage one. As shown in Fig. 2(c), the coal seam stored over 60 % of injected CO_2 by adsorption mechanism, which was tripled than it was in shale. However, owing to the unique rock heterogeneities from place to place, this result cannot reflect accurate quantitative comparisons between coal and shale. To compare with the *UF* of CO_2-ECBM with other processes, we normalized the *UF* from mass to energy basis. There were two key reasons that the energy basis was applied for comparison. First, the energy intensity contains great variability, which leads to an inconsistent comparison for different types of hydrocarbons. Second, the carbon footprint was commonly reported for operations on an energy basis. Thus, by translating to energy basis, it was instinctive to compare the emission reduction potential by geological carbon storage. According to Fig. 2(d), a largest UF_{net} was observed for CO_2-ECBM comparing with CO_2-ESGR with our previous work and CO_2-EOR with existing studies, demonstrating that the CO_2-ECBM operations can have the greatest carbon sequestration potential when providing the same magnitude of energy. Numerically, the UF_{net} in this study can reach to 0.08 $kgCO_2/MJ$ over the five years, and even greater as the project life expanded. Although the result demonstrated that CO_2-ECBM were able to sequester more CO_2

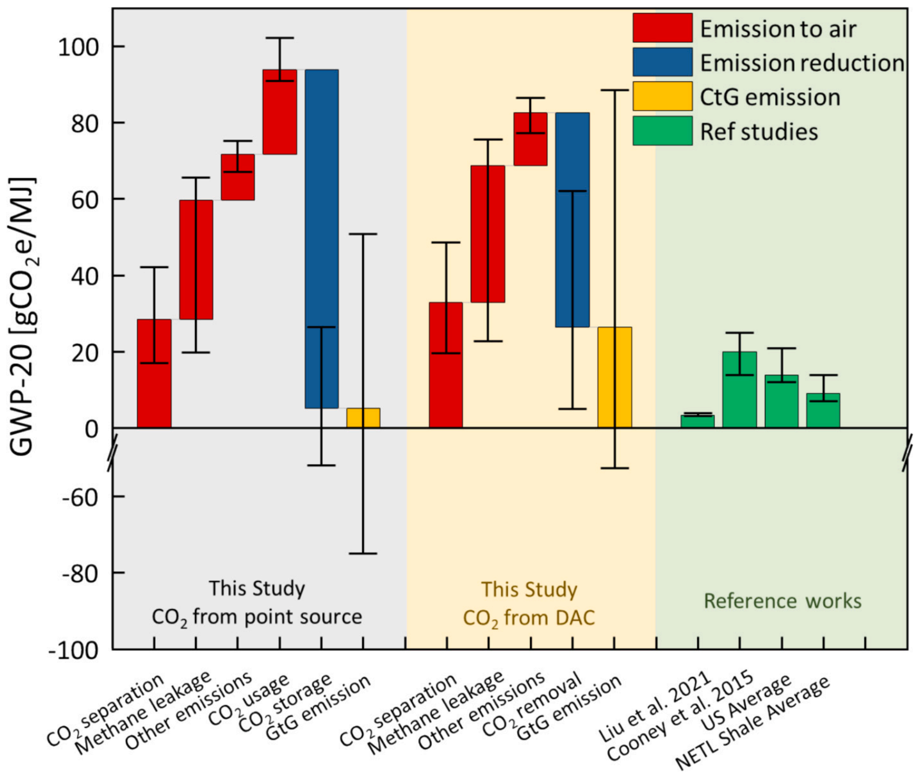

Fig. 4. The CtG GWP over 20-year timeframe breakdowns by process. In this study, we considered the CO_2 sourced from IC and DAC, as they are generating carbon offsets and removals, respectively. Error bars present the lower and upper estimates with the combinations of lower/upper values adapted from Table A1. Results have been compared with existing studies on natural gas and oil production from CO_2-EOR *and national emission factor inventories* on the energy basis (Liu et al., 2021; NETL, 2014). The conversion rate between gCO_2e/MJ to gCO_2e/$ of base case is 500 MJ/$ assuming the natural gas price at $2/GJ according to Table A1.

compared to other processes (i.e., doubled than CO_2-EOR), the expensive CO_2 cost and insufficient carbon policies avoided operators from investment on the large-scale CO_2-ECBMs. Therefore, the industrial revolution of reducing CO_2 supply cost and sufficient carbon policies would be necessitated in promoting the development of CO_2 sink in deep coal seams.

Concisely, this section presented utilizing CO_2 can recover an additional 8.5 % CBM through the permeability revolution and competitive adsorption mechanisms. Deep coal seams are ideal CO_2 storage medium owing to the large adsorption capacity, which provide reliable carbon storage potential, and can be reflected by the UF_{net}. In this study, 0.08 kg of CO_2 can be stored to deep coal seams while extracting 1 MJ of CBM (equivalent to 3.5 $kgCO_2$ per cubic meter of CBM on the mass basis) over the assumed project lifespan. In addition, compared with other CO_2 enhanced hydrocarbon recovery operations on an energy basis, more CO_2 can be stored during the operations. However, this has not been accepted by industry owing to the economic challenges.

3.2. Economic performance

In this section, annual CBM production and CO_2 retention are inputted into the DCF model such that the NPV and LCT can be determined. In Fig. 3(a), the breakdowns of NPV by earning and expense items are plotted. In this section, CO_2 was assumed to be sourced from the industrial capture process with pipeline transportation from the capture plant to the CBM field. As a considerable amount of CO_2 was successfully stored in the coal seam, approximately 70 % of earnings were generated by geological carbon storage, given the dynamic carbon tax increased annually. As a result, operations of CO_2-ECBM in this study can generate a total of $8.63 M monetary value over the five years' timeframe, where over half of the revenue is from geological carbon storage. Limitations exist as the uncertainties in drilling cost are underrepresented and we utilized a short project life owing to the sharp decline in CBM production rate. In practical, similar projects are expected to operate longer owing to the large CAPEX.

The LCT was another output from the TEA in this study as shown in Fig. 3(b), which measured the unit cost of producing 1 GJ of CBM during the project operation. Translating the LCT to the energy basis was to match the reported market price of natural gas, such that the cost-benefit analysis can be directly established. The LHV has been used for conversion purposes. As mentioned, owing to the dual functionalities of the CO_2-ECBM processes, the LCT has been allocated to the LCOM and LCOCS to represent the detailed costs for each functionality based on the revenue weighted factors. As a result, the LCT was estimated at $1.19 per GJ of CBM production associated with geological carbon storage. By applying the allocation, 76 % of LCT was attributed to the geological CO_2 storage, indicating that LCOCS was equivalent to $256/$tCO_2$, and the rest was belonging to the LCOM, which was $0.29/GJ. Comparing with Fig. 3(a), the percentage difference between revenue by each functionality versus the total earnings was caused by the salvage value of the equipment, which was excluded in the weighted function as it was not a recurring earning. The LCOCS was considerably beyond the current carbon tax even the price can reach to CAD 170 in Canada by 2030, it was still not affordable to stimulate the market growth of geological carbon storage in deep coal seams. However, the CO_2-ECBM can achieve profitability as the natural gas price was greater than the LCT. Operators are not intending to further implement the CO_2 sequestration in deep coal seams if CBM cannot guarantee the project profitability. Hence, stronger climate policies are crucial elements to commercialize the carbon storage pilots in coal seams.

3.3. Emissions and geological carbon storage

In this section, the CtG GWP of CO_2-ECBM was outlined combining

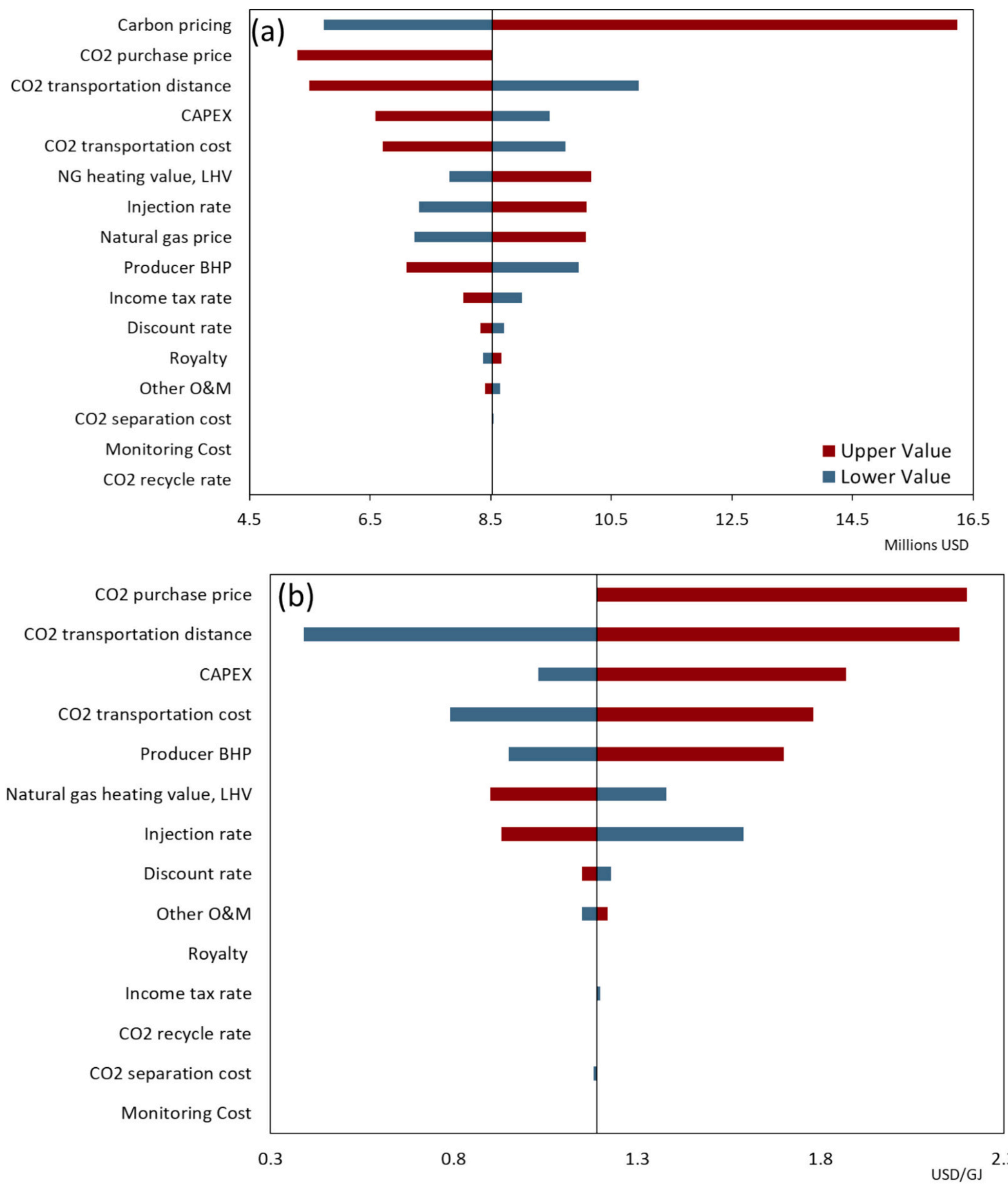

Fig. 5. Sensitivity analysis of (a) NPV, (b) LCT, (c) GtG GWP-20 with CO_2 from PSC, and (d) CtG GWP-20 with CO_2 from DAC. Lower/upper values are adopted from Table A1, (a) and (b) considers the economic plus operational parameters, while (c) and (d) considers environmental plus operational parameters. Varying operational parameters is carried out from the reservoir modeling by changing the corresponding conditions. Since we are conducting the site-specific case for the Manville CBM, the impact of geological inputs is excluded subsequently.

with CO_2 sourced either from industrial emitters or atmosphere. The results have been compared with pioneered studies as Fig. 4 exhibited (Cooney et al., 2015; Laurenzi and Jersey, 2013; Liu et al., 2021; NETL, 2014). When CO_2 sourced from the point source capture (PSC), the CI of CO_2 supply is positive as the capturing process generated GHG emissions, which left uncaptured amount release to atmosphere given the capture efficiency (i.e. up to 99 %, we assumed a conservative rate of 90 % in this study) of the configurations (Müller et al., 2020). Therefore, the CtG net GHG emissions (Eq. (15)) can be modified as follows (Eq. (16)).

$$E_T = E_{upstream} + E_{CO_2-ECBM} = E_{uncaptured} - E_{capture} \times R_{CO_2,ret} + E_{operation} \tag{16}$$

The net emissions contained the operational emissions during CO_2-ECBM plus the uncaptured industrial emissions and the abatement of geological CO_2 storage. The breakdowns for each unit process were described in the grey region in Fig. 4. As shown, major contributions of emissions were from methane leakage, CO_2 separation and uncaptured CO_2 during the upstream segment. We assumed a 2 % leakage rate in our base scenario, it still has a significant contribution to final estimate owing to the greater GWP of methane. Similarly, the CO_2 separation is a high energy intensive process that consumed considerable electricity, which causing the largest portion of GWP for the CO_2-ECBM process. The advantage of CO_2 retention is to counterbalance the GHG emissions for the CO_2-ECBM process, which demonstrated exceptional ability to neutralize all emissions produced inside the CtG system boundaries. Nevertheless, the presence of a negative value does not imply that negative-carbon CBM can be generated by the CO_2-ECBM process, since the CO_2 used in this process is obtained from PSC. The interpretation of a negative value is that GHG emissions can be eliminated over the whole life cycle, from cradle-to-grave. The most optimistic estimate is that

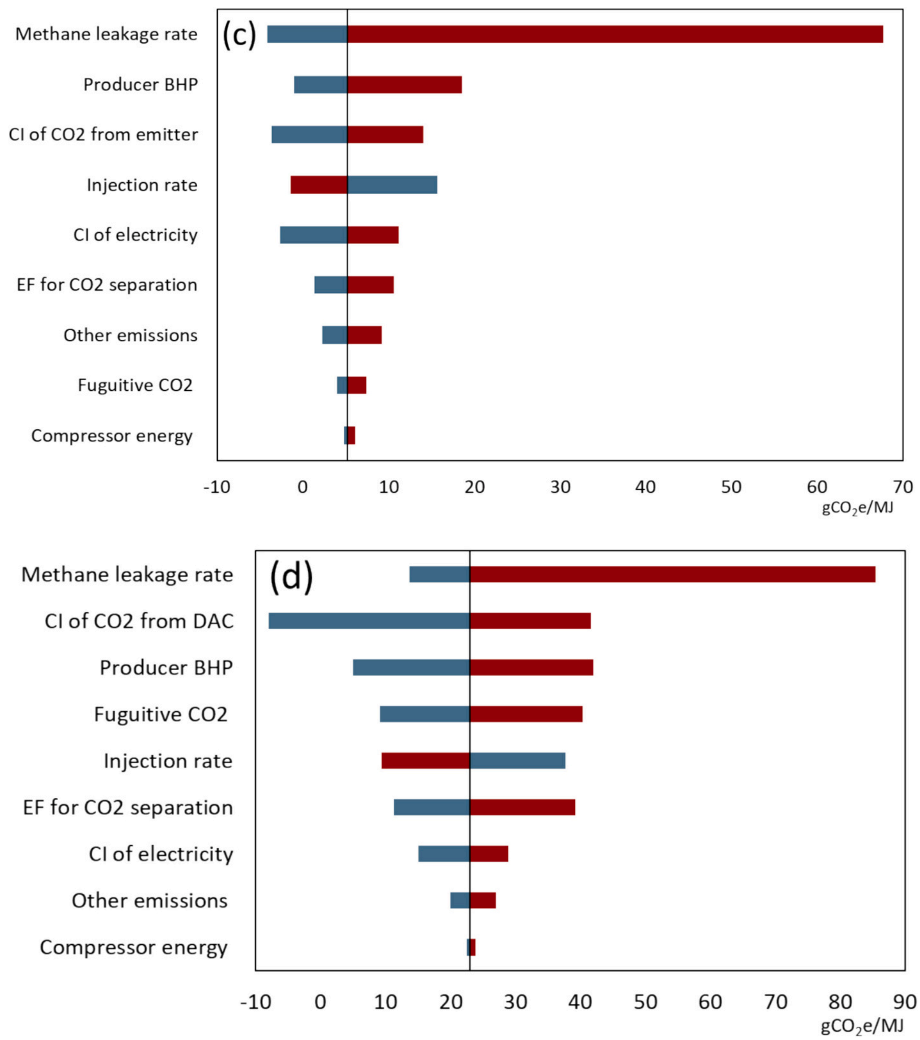

Fig. 5. (*continued*).

emissions can be reduced to net-zero if all emissions from the downstream segment can be neutralized. By comparing with previous studies (see green region in Fig. 4), Liu et al. documented natural gas produced in Western Canada can generate GHG emissions at the magnitude of 3.1 to 4 gCO_2eq/MJ, which specifically focused on the primary recovery process for the conventional reservoirs (Liu et al., 2021). Due to the energy-intensive nature of the CO_2 supply and field application process, any alterations in the carbon intensity of energy supply can lead a considerable impact on the scope 2 emissions for the CtG CO_2-ECBM. Hence, the primary disparities can be ascribed to the use of carbon dioxide in this study. This study showed that geological carbon sequestration is essential for CO_2-ECBM to produce environmentally comparable alternatives to current approaches. Furthermore, Cooney et al. observed that crude oil production from CO_2-EOR can result in the generation of >30 to 58 gCO_2e/MJ if excluding the advantages of CO_2 mitigation. This is 2 to 3 times greater than that of conventional crude oil production as determined by NETL (Cooney et al., 2015). In this study, we found that the CO_2 field application can raise GHG emissions for the CO_2-ECBM, which is consistent with previous literature. However, it is concluded that geological CO_2 storage has a greater potential to reduce those emissions in CO_2-ECBM compared to CO_2-EOR. Due to the reliance on reservoir modeling results, conducting uncertainty analysis will require in-depth information on geological features at the site-level, which raises the limitations of this work.

When CO_2 sourced from the DAC and permanently stored to the subsurface porous media, which also known as carbon dioxide removal (CDR) (USDOE, 2023). As such, the CtG GWP of CO_2-ECBM can be adjusted as Eq. (17).

$$E_T = E_{upstream} + E_{CO_2-ECBM} = -\left(M_{DAC} \times eff_{CDR}\right) \times R_{CO_2} + E_{operation} \tag{17}$$

where M_{DAC} is the total amount of CO_2 captured from air on the mass basis, and eff_{CDR} is the CDR efficiency defined by $eff_{CDR} = M_{DAC} - E_{DAC}/M_{DAC}$, where E_{DAC} is the associated GHG emissions for the deployment of DAC (Müller et al., 2020). The negative sign of CI for CO_2 supply from DAC means that CO_2 is removed from air (Sievert et al., 2024). As demonstrated in Fig. 4, it is observed that the CtG GWP was 23, ranging from −60 to 85 g/MJ, which surpassed the scenario using CO_2 from point sources. Similar as the DACS (refer to DAC with carbon storage), it revealed that negative-carbon CBM is possible once the end-use emissions can be covered by geological carbon storage (Tanzer and Ramírez, 2019). In the reservoir modeling of this study, we observed that CO_2 can be continuously injected into the deep coalbed, but the cost of DAC CO_2 will be a major concern, which ceased the project as it was not economically profitable. As reported, future large-scale deployment of DAC will be ranged from \$160 to \$280/tCO_2. With the depletion of daily CBM production rate, rising amount of CO_2 will be injected and stored to the reservoir, and UF_{net} curve will increase, indicating that more CO_2 will be stored associated with same amount of CBM production. As CO_2 was sourced from atmosphere, the CO_2-ECBM demonstrated a growing capability of producing negative-carbon CBM on the

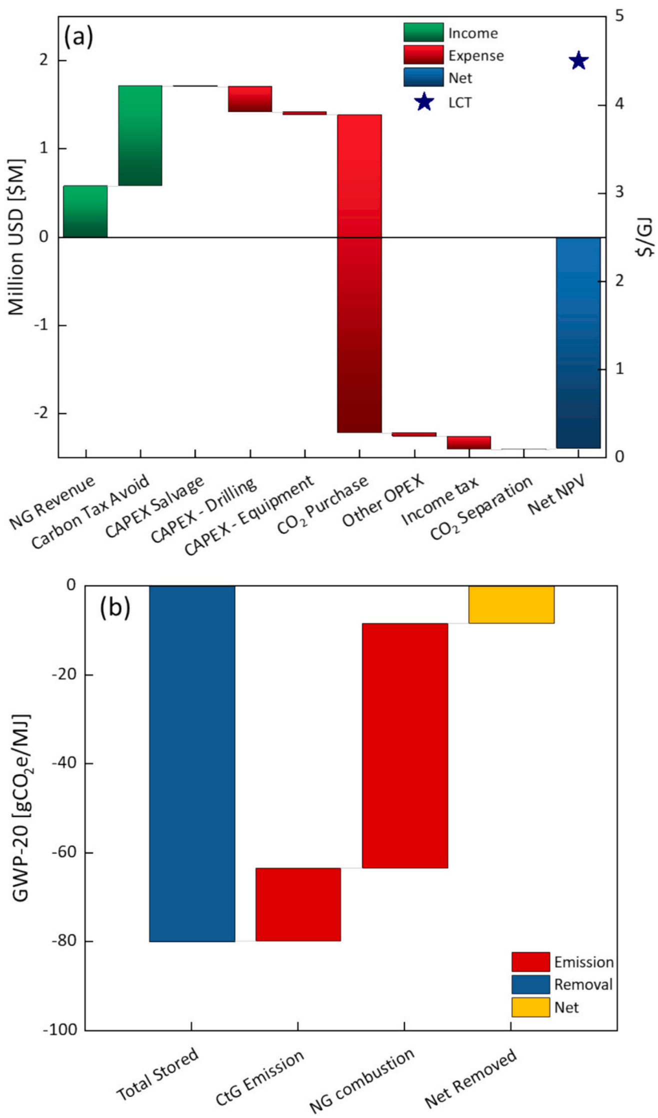

Fig. 6. Integrated TEA and LCA analysis of DAC-CO_2-ECBM. Assumptions include the cost of DAC at \$200/tCO_2 at the CDR rate of −600 gCO_2e/kg (Table A1), indicating that per kg of CO_2 removed can generate 400 gCO_2e emissions. Data can be retrieved from the existing literature (Müller et al., 2020). (a) describes the breakdown of NPV and the LCT (the blue star on the very right column, right *y*-axis) estimate based on the DCF model in this work. (b) highlights the CO_2 storage associated with emissions during the CO_2-ECBM, while the combustion emission is assumed at a conservative case with the emission factor retrieved from U.S. energy information administration (EIA) at 55 gCO_2e/MJ (USEIA, 2021).

time horizon. As such, it was recommended to consider geological CO_2 storage as the co-product at the early stage, and CBM as the co-product at the late stage, which can influence the decision-making strategy of CO_2-ECBM. In short, we revealed that delivering negative-carbon CBM is achievable, but the LCA system boundary must cover the downstream segment. The expensive cost of DAC is the primary deterrent for operators considering DACS during CO_2-ECBM. Implementing robust climate policies and reducing the DAC cost can stimulate the industrial expansion of CO_2-ECBM paired with DAC technology.

3.4. Sensitivity analysis

We performed the one-at-a-time sensitivity analysis on a total of sixteen and nine variables respectively to assess their individual effects TEA and LCA. Fig. 5 illustrates the influence of each parameter on the TEA, with (a) and (b) representing the NPV and LCT correspondingly. Additionally, Fig. 5(c) and (d) depicts the impact on the LCA in terms of CO_2 supplied by PSC and DAC. Our findings indicate that the carbon tax rate had the greatest impact on the NPV due to the fact that >70 % of the income was obtained from the geological carbon storage through CO_2-ECBM. Given the consideration of the expensive cost of CO_2 from DAC, the CO_2 purchase price had a significant impact on both NPV and LCT. Regarding the LCA findings, we discovered that methane emission was the primary influencing element, irrespective of the sources of CO_2, due to its significant GWP. Nevertheless, the methane leakage rate in this study was derived from assumptions made according to the GHG inventory report, which may be significantly underestimated based on previous research (Alvarez et al., 2018; Yang et al., 2024). Other factors were demonstrated to have comparable rankings for both LCA as shown in Fig. 5(c) and (d).

3.5. Trade-offs of negative-carbon CBM

In this section, we integrated the TEA and LCA for CO_2-ECBM, assuming CO_2 sourced from DAC to evaluate the economic and environmental trade-offs for delivering the negative-carbon CBM. In Fig. 6 (a) and (b), the TEA and LCA were performed by the 3E analytical model developed in this investigation. As a result, the CO_2-ECBM cannot be profitable by deploying CO_2 from DAC, owing to the expensive cost (see Fig. 6(a), CO_2 purchase account for over 90 % of total cost). The LCT was calculated at \$4.7/GJ, which is about 4 times higher (increased marginal LCT by \$3.5/GJ in magnitude) than it was coupling with PSC CO_2. On the other hand, by incorporating the end-use emission, where we assumed a simple combustion case, but methane can always be used for producing value-added petrochemicals through the chemical upgrading processes, it showed that a net of 8.6 g CO_2 can be permanently removed per producing 1 MJ of CBM over the project lifespan. Physically, the finding indicated that the entire process resulted in a net CDR efficiency of 6.2 %, as it required a total of 130 g CO_2 capturing from DAC at the DAC eff_{CDR} of 60 %. Importantly, the marginal levelized cost of CDR can be calculated at \$407/tCO_2 for the CO_2-ECBM process. By performing the breakeven analysis using the 3E model, we concluded that either the carbon tax rate reach to \$175/tCO_2 or the DAC CO_2 price decreased to below \$115/tCO_2 will be required to make the CO_2-ECBM profitable. Alternatively, the CDR efficiency was required to reach 86 % to produce the net zero-carbon CBM at the current market conditions, indicating that a −860 gCO_2e/kg CO_2 supply is necessitated.

4. Conclusion

In this investigation, we introduced a 3E system analytical framework for the CO_2-ECBM process at the system level based on the reservoir modeling, TEA and LCA approaches of the Manville coal. Tackling the knowledge gaps to stimulate the field application, we established the performance evaluation matrix for decision-making at the early stage. Additionally, with CO_2 supplied from different sources, the proposed 3E framework was applied to identify the conditions to deliver net-zero-carbon and negative-carbon CBM based on the simulations. Findings of this study offer multi-disciplinary urgent support for operators, investors, and policymakers in assessing the economic and environmental benefits of CO_2-ECBM as well as improving climate policies to support CDR. Four key findings are summarized below.

First, the reservoir simulation revealed that a total of 8.5 % CBM can be recovered by CO_2 injection, and 99 % of injected CO_2 can be stored permanently to the deep Manville coal seam through the adsorptive and the structural trapping mechanisms. Unlike other depleted hydrocarbon reservoirs, over 60 % of CO_2 storage capacity was created by the adsorption, which provided secured GHG emission reduction opportunities. The net utilization factor of CO_2-ECBM was calculated at 0.08 kg/MJ, meaning that 0.08 kg CO_2 was stored associated with 1 MJ of natural gas production, which was potentially twice as great as the net utilization factors for the CO_2-EOR process. However, it also implied that a larger amount of CO_2 must be purchased compared to CO_2-EOR for supplying the same amount of energy, leading to a diminishing return for the implementation of CO_2-ECBM.

Second, our 3E analytical framework estimated the levelized cost of CBM production at \$1.19/GJ comprised of LCOCS of \$256/tCO_2 and \$0.19/GJ CBM production by revenue allocation. The CtG GWP was determined to range from −75 to 82 gCO_2e/MJ, where the negative meaning differently depending on the sources of CO_2 supply. Although application of CO_2 can generate a larger GWP of CBM production than conventional natural gas production, the excessive emissions can be completely eliminated by taking advantage of geological CO_2 sequestration. Methane emissions are primarily GWP drivers, but the current GHG inventories are under-reported, resulting in ambiguity in our calculations.

Third, when CO_2 is from industrial sources, the optimal scenario is to produce the carbon-neutral CBM throughout the entire CO_2-ECBM life cycle, from cradle to grave. Eventually, the uncaptured CO_2 from upstream, end-use emissions from downstream segments, and all operational emissions across the entire life cycle need to be geologically stored during the CO_2-ECBM operations. As such, the net-zero-carbon CBM can be delivered at the gate, which is achievable under the current technology constrictions.

Fourth, when CO_2 is from atmosphere, it is possible to deliver the negative carbon CBM but at a much higher cost. Specifically, the total levelized cost was evaluated at \$4.7/GJ CBM delivery associated with 8.6 g CO_2 removal, resulting in a net CDR efficiency of 6.2 %. Given the existing market and environmental conditions, there are two ways to enable DAC-CO_2-ECBM to be profitable. From the economic perspective, we need to either reduce the DAC cost to approximately \$115/tCO_2 or increase the carbon tax rate to \$175/tCO_2 conservatively. From the environmental perspective, we need to improve the efficiency of DAC to at least 86 % so that the CO_2 can be supplied at the intensity of −860 gCO_2e/kg.

Supplementary data to this article can be found online at https://doi.org/10.1016/j.scitotenv.2025.178721.

CRediT authorship contribution statement

Haoming Ma: Writing – review & editing, Writing – original draft, Visualization, Validation, Software, Resources, Project administration, Methodology, Investigation, Formal analysis, Data curation, Conceptualization. **Yun Yang:** Writing – review & editing, Writing – original draft, Visualization, Validation, Software, Formal analysis, Data curation, Conceptualization. **Zhenqian Xue:** Writing – review & editing. **Christopher R. Clarkson:** Writing – review & editing, Formal analysis, Data curation, Conceptualization. **Zhangxin Chen:** Writing – review & editing, Supervision, Software, Resources, Project administration, Methodology, Data curation, Conceptualization.

Declaration of competing interest

The authors declare that there are no known competing financial interests or personal relationships that could have appeared to influence the work reported in this paper.

Acknowledgements

This research has been made possible by contributions from the Natural Sciences and Engineering Research Council (NSERC)/Energi Simulation Industrial Research Chair in Reservoir Simulation, the Alberta Innovates (iCore) Chair in Reservoir Modelling, and the Energi Simulation/Frank and Sarah Meyer collaboration Centre.

Data availability

Data will be made available upon request. Appendix table of data assumptions is available in supporting information.

References

Abuov, Y., Serik, G., Lee, W., 2022. Techno-economic assessment and life cycle assessment of CO2-EOR. Environ. Sci. Technol. 56, 8571–8580.

Alberta Energy Regulator, 2023. Alberta Natural Gas Reference Price.

Alvarez, R.A., Zavala-Araiza, D., Lyon, D.R., Allen, D.T., Barkley, Z.R., Brandt, A.R., et al., 2018. Assessment of methane emissions from the U.S. oil and gas supply chain. Science 361, 186–188.

Azzolina, N.A., Peck, W.D., Hamling, J.A., Gorecki, C.D., Ayash, S.C., Doll, T.E., et al., 2016. How green is my oil? A detailed look at greenhouse gas accounting for CO2-enhanced oil recovery (CO2-EOR) sites. Int. J. Greenhouse Gas Control 51, 369–379.

Brandt, A.R., Masnadi, M.S., Rutherford, J., Englander, J., 2022. OPGEE Model.

Bui, M., Adjiman, C.S., Bardow, A., Anthony, E.J., Boston, A., Brown, S., et al., 2018. Carbon capture and storage (CCS): the way forward. Energy Environ. Sci. 11, 1062–1176.

Canadian Institute of Mining, Metallurgy and Petroleum, 2024. Historical Canadian Mines Data.

Chen, Z., 2007. Reservoir Simulation Mathematical Techniques in oil Recovery. Society for Industrial and Applied Mathematics.

Clarkson, C.R., Jordan, C.L., Gierhart, R.R., Seidle, J.P., 2008. Production data analysis of coalbed-methane wells. SPE Reserv. Eval. Eng. 11, 311–325.

Computer Modeling Group, Ltd. CMG-GEM, 2020. [Computer Software], Calgary, AB Canada.

Cooney, G., Littlefield, J., Marriott, J., Skone, T.J., 2015. Evaluating the climate benefits of CO2-enhanced oil recovery using life cycle analysis. Environ. Sci. Technol. 49, 7491–7500.

Dahi Taleghani, A., Cai, Y., Pouya, A., 2020. Fracture closure modes during flowback from hydraulic fractures. Int. J. Numer. Anal. Methods Geomech. 44, 1695–1704.

El-Houjeiri, H.M., Brandt, A.R., Duffy, J.E., 2013. Open-source LCA tool for estimating greenhouse gas emissions from crude oil production using field characteristics. Environ. Sci. Technol. 47, 5998–6006.

Environment and Climate Change Canada, 2023. The Greenhouse Gas Intensity of Canada's Electricity Grid 2023.

Environmental Defense Fund, 2015. Leak Detection and Repair Cost Effectiveness Analysis.

Fukai, I., Mishra, S., Moody, M.A., 2016. Economic analysis of CO2-enhanced oil recovery in Ohio: implications for carbon capture, utilization, and storage in the Appalachian Basin region. Int. J. Greenhouse Gas Control 52, 357–377.

Gong, Y., Mehana, M., El-Monier, I., Viswanathan, H., 2020. Proppant placement in complex fracture geometries: a computational fluid dynamics study. J. Nat. Gas Sci. Eng. 79, 103295.

Government of Alberta, 2024. Royalty Overview.

Gunter WD, Mavor MJ, Law DH-S. Process for recovering methane and/or sequestering fluids. Google Patents, 2002.

Heath, G.A., O'Donoughue, P., Arent, D.J., Bazilian, M., 2014. Harmonization of initial estimates of shale gas life cycle greenhouse gas emissions for electric power generation. Proc. Natl. Acad. Sci. USA 111, E3167–E3176.

Hughes, S., Zoelle, A., Woods, M., Henry, S., Homsy, S., Pidaparti, S., et al., 2022. Cost of Capturing CO2 From Industrial Sources. National Energy Technology Laboratory (NETL), United States.

International Energy Agency, 2022a. Canada 2022 Energy Policy Review. IEA, Paris.

International Energy Agency, 2022b. Direct Air Capture. IEA, Paris.

International Energy Agency, 2023a. CCUS Policies and Business Models.

International Energy Agency, 2023b. Energy Technology Perspectives. IEA, Paris.

International Energy Agency, 2024. World Energy Outlook 2024.

IPCC, 2023. Climate Change 2023 Synthesis Report.

ISO14040, 2006. Environmental Management - Life Cycle Assessment Principles and Framework. European Committee for Standardisation (ISO 14040:2006).

ISO14044, 2006. Environmental Management – Life Cycle Assessment – Requirements and Guidelines. European Committee for Standardisation (ISO 14044:2006).

ISO14067, 2018. Greenhouse Gases — Carbon Footprint of Products — Requirements and Guidelines for Quantification. European Committee for Standardization (ISO 14067:2018).

Jiang, J., Rui, Z., Hazlett, R., Lu, J., 2019. An integrated technical-economic model for evaluating CO2 enhanced oil recovery development. Appl. Energy 247, 190–211.

Kolster, C., Masnadi, M.S., Krevor, S., Mac Dowell, N., Brandt, A.R., 2017. CO2 enhanced oil recovery: a catalyst for gigatonne-scale carbon capture and storage deployment? Energy Environ. Sci. 10, 2594–2608.

Laurenzi, I.J., Jersey, G.R., 2013. Life cycle greenhouse gas emissions and freshwater consumption of Marcellus shale gas. Environ. Sci. Technol. 47, 4896–4903.

Littlefield, J., Augustine, D., Pegallapati, A., Zaimes, G.G., Rai, S., Cooney, G., et al., 2019. Life Cycle Analysis of Natural Gas Extraction and Power Generation. National Energy Technology Laboratory (NETL).

Liu, R.E., Ravikumar, A.P., Bi, X.T., Zhang, S., Nie, Y., Brandt, A., et al., 2021. Greenhouse gas emissions of Western Canadian natural gas: proposed emissions tracking for life cycle modeling. Environ. Sci. Technol. 55, 9711–9720.

Lu, C., Xiao, X., Xue, Z., Chen, Z., Li, G., Feng, Y., 2023. Fractal and multifractal characteristics of nanopores and their controlling factors in marine–continental

transitional shales and their kerogens from Qinshui Basin, Northern China. Nat. Resour. Res. 32, 2313–2336.
Ma, H., 2023. Data-driven Carbon Dioxide Enhanced Oil Recovery Models and Their Applications (PhD Dissertation). University of Calgary, Calgary, Alberta Canada.
Ma, H., Chen, S., Xue, D., Chen, Y., Chen, Z., 2021. Outlook for the coal industry and new coal production technologies. Adv. Geo-Energy Res. 5, 119–120.
Ma, H., Yang, Y., Zhang, Y., Li, Z., Zhang, K., Xue, Z., et al., 2022. Optimized schemes of enhanced shale gas recovery by CO2-N2 mixtures associated with CO2 sequestration. Energy Convers. Manag. 268.
Masnadi, M., El-Houjeiri, H., Schunack, D., Li, Y., Englander, J., Badahdah, A., et al., 2018a. Global carbon intensity of crude oil production. Science (AAAS) 361, 851–853.
Masnadi, M.S., El-Houjeiri, H.M., Schunack, D., Li, Y., Roberts, S.O., Przesmitzki, S., et al., 2018b. Well-to-refinery emissions and net-energy analysis of China's crude-oil supply. Nat. Energy 3, 220–226.
McCoy, S., Rubin, E., 2008. An engineering-economic model of pipeline transport of CO2 with application to carbon capture and storage. Int. J. Greenhouse Gas Control 2, 219–229.
Moore, T.A., 2012. Coalbed methane: a review. Int. J. Coal Geol. 101, 36–81.
Müller, L.J., Kätelhön, A., Bringezu, S., McCoy, S., Suh, S., Edwards, R., et al., 2020. The carbon footprint of the carbon feedstock CO2. Energy Environ. Sci. 13, 2979–2992.
National Energy Technology Laboratory, 2014. Life Cycle Analysis of Natural Gas Extraction and Power Generation.
NIH, 2024. PubChem Compound Summary for CID 280, Carbon Dioxide.
Sievert, K., Schmidt, T.S., Steffen, B., 2024. Considering technology characteristics to project future costs of direct air capture. Joule 8 (4), 979–999.
Sleep, S., Munjal, R., Leitch, M., Extavour, M., Gaona, A., Ahmad, S., et al., 2021. Carbon footprinting of carbon capture and -utilization technologies: discussion of the analysis of Carbon XPRIZE competition team finalists. Clean Energy 5, 587–599.
Tanzer, S.E., Ramírez, A., 2019. When are negative emissions negative emissions? Energy Environ. Sci. 12, 1210–1218.
United States Department of Energy, 2023. Roads to Removal: Options for Carbon Dioxide Removal in the United States.
United States Energy Information Administration, 2021. Carbon Dioxide Emissions Coefficients.
von der Assen, N., Voll, P., Peters, M., Bardow, A., 2014. Life cycle assessment of CO2 capture and utilization: a tutorial review. Chem. Soc. Rev. 43, 7982–7994.
Xue, Z., Ma, H., Sun, Z., Lu, C., Chen, Z., 2024a. Technical analysis of a novel economically mixed CO2-water enhanced geothermal system. J. Clean. Prod. 448, 141749.
Xue, Z., Ma, H., Wei, Y., Wu, W., Sun, Z., Chai, M., et al., 2024b. Integrated technological and economic feasibility comparisons of enhanced geothermal systems associated with carbon storage. Appl. Energy 359.
Xue, Z., Zhang, Y., Ma, H., Lu, Y., Zhang, K., Wei, Y., et al., 2024c. A combined neural network forecasting approach for CO2-enhanced shale gas recovery. SPE J. 29, 4459–4770.
Yang, Y., Liu, S., Clarkson, C., 2022. Quantification of temperature-dependent sorption isotherms in shale gas reservoirs: experiment and theory. SPE J. 1–19.
Yang, Y., Clarkson, C.R., Hamdi, H., Ghanizadeh, A., Blinderman, M.S., Evans, C., 2023a. Field pilot testing and reservoir simulation to evaluate processes controlling CO2 injection and associated in-situ fluid migration in deep coal. Int. J. Coal Geol. 275.
Yang, Y., Hamdi, H., Clarkson, C.R., Blinderman, M.S., 2023b. Numerical modeling of field pilot data designed to evaluate CO2 storage potential in the deep Mannville coal seams of Alberta. In: SPE Canadian Energy Technology Conference and Exhibition.
Yang, Y., Liu, S., Ma, H., 2024. Impact of unrecovered shale gas reserve on methane emissions from abandoned shale gas wells. Sci. Total Environ. 913, 169750.